Materials Science & Engineering A 737 (2018) 310–317

Contents lists available at ScienceDirect

Materials Science & Engineering A

journal homepage: www.elsevier.com/locate/msea

A new recrystallization at semi-coherent micro-lamella and its effect on tensile properties of wire arc additive manufactured titanium alloy

Yong Xie, Ming Gao*, Fude Wang, Quan Li, Xiaoyan Zeng

Wuhan National Laboratory for Optoelectronics (WNLO), Huazhong University of Science and Technology, Wuhan 430074, PR China

ARTICLE INFO

Keywords:
Recrystallization
Additive manufacturing
Micro-lamella
Semi-coherent interface
Tensile properties

ABSTRACT

A new recrystallization without plastic deformation was observed at the semi-coherent micro-lamella (ML) of wire arc additive manufactured Ti6Al4V, which is driven by the interface energy and the dislocation-induced elastic strain energy. It was classified into three types according to nucleation site, which are the recrystallization at the boundary of colony structures, inside the colony structures, and at the boundary of basket weave structures, respectively. Some new behaviors in the nucleation and growth of this recrystallization were found. Firstly, the nucleation mechanism of one direction strain and interface induced grain boundary migration was found in the recrystallizations at colony boundary and inside the colony. Secondly, the recrystallized grains at colony boundary grew to be part of the original colony, while the others grew to be a new grain. Relevant mechanisms were discussed according to theoretical calculation of driving energy and grain growth behaviors. Because the continuous grain boundaries were broken by this recrystallization, not only the ultimate tensile strength was increased by 100 MPa or so, but also the ductility anisotropy was decreased from the 4.8% of as-deposited sample to the 0.2%. The results would provide a new approach without plastic deformation to improve the performances of additive manufactured components.

1. Introduction

Wire arc additive manufacturing (WAAM) is one of the most important techniques to fabricate large scale components due to high deposition rate and low cost [1–3]. WAAMed Ti6Al4V was usually featured by coarse columnar grains and continuous α grain boundaries (α_{GB}) epitaxially growing to pass through deposited layers [4,5]. It caused the anisotropy, and decreased the mechanical properties to lower than those of rolled and forged components [6,7]. How to solve these problems has been one of the most significant challenges for WAAMed Ti6Al4V.

Introducing plastic deformation to induce the recrystallization and destroy the continuity of α_{GB} is an effective technique to improve the mechanical properties of WAAMed titanium (Ti) alloys [1,8,9]. Maritina et al. and He et al. had destroyed the continuous α_{GB} of WAAMed Ti6Al4V by employing the layer-by-layer rolling and ultrasonic impacting [10,11]. However, the extra processes decreased the deposition efficiency, and increased the cost because of the difficult implementation. Presently, Vovk et al. reported a nano-lamellar recrystallization without plastic deformation in giant magneto-resistance multilayer systems [12–14], driven by the elastic strain energy and induced by the lattice mismatch between the coherent interface where the atoms and planes across the interface between two crystal structures is completely continuous [15]. Guyon et al. found the nano-lamellar recrystallization in TiAl alloy, driven by twin-induced coherent interface energy and elastic strain energy [16].

In current study, a new recrystallization at the micro-lamellar (ML) with semi-coherent interface, where the disregistry across the interface between two crystal structures is accommodated by periodic misfit dislocations in the interface [15], was presented. It occurred without any plastic deformation, and just needed a temperature higher than recrystallization temperature. The nucleation and growth behaviors of this recrystallization were presented and discussed in detail.

2. Experimental procedures

The WAAM equipment was composed of a Fronius MagicWave 4000 plasma welder and a Fanuc M-710iC robot. The deposition material was 1.2 mm-diameter Ti6Al4V wire with the chemical compositions (wt%) of Al6.1-V4.0-Fe0.15-C0.01-N0.01-H0.002-O0.16-Ti balance. The substrate was hot rolled Ti6Al4V plate with the size of $400 \times 400 \times 20\ mm^3$ (Length × Width × Thickness). The experiment was shielded by pure argon. In order to prevent the oxidation, each layer was deposited when the temperature of previous layer was below

* Corresponding author.
E-mail address: mgao@mail.hust.edu.cn (M. Gao).

https://doi.org/10.1016/j.msea.2018.09.076
Received 21 July 2018; Received in revised form 19 September 2018; Accepted 20 September 2018
Available online 21 September 2018
0921-5093/

100 °C. The deposition was carried out by reversed deposition direction. The parameters were the arc current of 115 A, the wire feed speed of 1.6 m/min, the deposition speed of 0.18 m/min, the vertical build interval of 1.1 mm, and the interlayer spacing time of 180 s. The final size of the deposited thin-wall was 380 × 145 × 20 mm^3.

The heat treatment was carried out in a SRJX-4-13 box furnace with a heating rate of 5 °C/min. The β transfer temperature was tested by TGA-STA449F3 equipment, which is 960 ± 5 °C. The heat treatment procedure was carried out at the temperature of 900 °C for 2 h and water-cooled. Before the testing, a cylinder sample with 3 mm-diameter and 2 mm-thickness was cut and prepared to detect the oxygen content by a Bruker G8 GALILEO equipment. It demonstrated that the oxygen content was less than 0.2%, which is in accord with the standard of ASTM B367-13.

According to above oxygen test results, each side of all samples was milled by 1.5 mm-thickness before testing in order to avoid the effect of surface oxide. The metallographic samples were prepared by two steps. Firstly, the out layer of the thin-wall was removed by 1.5 mm-thick. Secondly, the metallographic samples were taken from the milled part in the region below the top of 5 mm and above the bottom of 2 mm, as shown in Fig. 1. The microstructure observation surface was XZ plane. The samples were etched by the solution of 1 ML HF, 6 ML HNO_3 and 100 ML H_2O for 30 s. The microstructure was observed by scanning electron microscopy (SEM, FEI Nova SEM 450), electron backscattered diffraction (EBSD, FEI Sirion 200) with the step size of 0.15 μm, and transmission electron microscopy (TEM, FEI Tecnai G2 F30). The TEM sample was a 3 mm-diameter thin foils, double spray electrolysis polished by the reagent of 6% $HClO_4$, 34% $CH_3CH_2CH_2CH_2OH$ and 60% CH_3OH (in vol.).

3. Results

3.1. Microstructure of as-deposited Ti6Al4V

As shown in Fig. 2a, the microstructure of as-deposited Ti6Al4V is characterized by the colony structure and the basket weave structure at the sides of α_{GB}. The colony is characterized by some parallel ML grains, including micro-lamellar α phase (ML-α) and micro-lamellar β phase (ML-β). The average width of the colony is about 9.4 μm. The basket weave is characterized by some staggered ML grains. As shown in Fig. 3, the average width of ML-α is about 1.22 μm, while that of dark ML-β between the ML-α grains is about 0.08 μm. Fig. 2b is an inverse pole figure (IPF) of Fig. 2a, which plots the grain orientation of a given specimen direction with respect to the crystal axes. It shows that the fraction of the large angle grain boundary with the angle more than 5°, also called high grain boundary [15], is 95.7%. The α/β interface is in accord with the Burges orientation relationship (BOR) of $(0001)_\alpha$// $(110)_\beta$ and $[-2110]_\alpha$//$[-11-1]_\beta$, which is with the misorientation of 10.5°. According to the interface definition in ref. [17,18], the α/β interface can be confirmed as the semi-coherent interface.

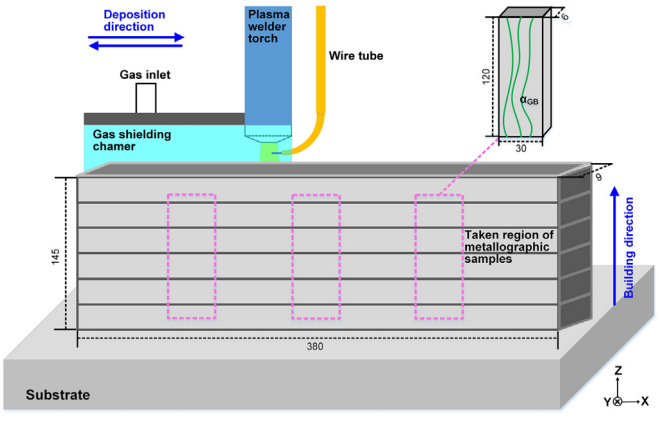

Fig. 1. Schematic drawing of experimental set-up and the taken position of metallographic sample.

As shown in Fig. 3a, the dislocation density is different at the sides of colony boundary. Lots of screw dislocations pass through the colony boundary to the adjacent colony, which causes the dislocation pile-up at the semi-coherent interface. Fig. 3b shows the narrow ML-α has higher dislocation density than the wide one because a large amount of dislocation intercepts and steps pass through it. As shown in Fig. 3c, the ML-α grains in the basket weave stagger each other by a certain curvature, causing serious dislocation pile-up at the boundary and inside the ML-α. As shown in Fig. 3d, some dislocation loops are found at the staggered interface [19].

This microstructure characteristics denote that the semi-coherent interface and the dislocation pile-up could be formed by the thermal stress resulted from the fast cooling rate and the big thermal cycle in WAMM process. It causes the mismatch at the semi-coherent interface, and would provide the necessary driving energy for recrystallization, which will be discussed in following sections.

3.2. Recrystallization microstructure

As shown in Fig. 4a, the microstructure of heat-treated Ti6Al4V is composed of equiaxed α phase, α' phase and the colony. Both the α' phase and the colony pass through the α_{GB}. The volume fractions of the equiaxed α and α' are 3% and 5%, respectively. Similar to the ref [14,16], the grain color in the IPF was selected as the criterion to confirm the recrystallized grains. As the appointed areas of I, II and III in Fig. 4b, some recrystallized grains appear at the colony boundary, inside the colony and at the basket weave boundary, respectively. It is different with the conventional viewpoint that the recrystallization cannot occur in WAAMed Ti6Al4V without plastic deformation [20].

As shown in Fig. 5a, the recrystallized grains at the colony boundary, Re-α1 and Re-α2 nucleate at the boundary of the ML-α1 (also the colony boundary), and grow up by swallowing the ML-α grains in adjacent colony. The growth interface is curved, indicating the recrystallized grains grow at a certain curvature rather than along the colony boundary uniformly. Balachandran et al. and Zhao et al. suggested that the large misorientation at the colony boundaries has high interface energy, and benefits the curved growth [21,22]. Fig. 5b shows the misorientation between ML-α1 and Re-α1, Re-α2 are 1° and 3°, respectively. Both of them are less than 5°. It denotes that these recrystallized grains have the same BOR with original ML-α, and are part of the original colony.

As shown in Fig. 6a, the recrystallized grain inside the colony, Re-α3 grows up along the boundary of ML-α2 with curved interface. The horizontal width of Re-α3 is 3.38 μm, larger than the average width of ML-α (1.22 μm) by two times or so. It indicates that the recrystallized grain passes through several ML-α grains, and grows up by swallowing them. Fig. 6b shows the misorientation between Re-α3 and ML-α2 is 45.2°, far larger than 5°. It suggests that Re-α3 has no BOR with original ML-α, and is a new grain.

As shown in Fig. 7a, the recrystallized grains at the basket weave boundary, Re-α4 grows to an equiaxed grain by swallowing adjacent ML-α grains (ML-α5 , ML-α6 , ML-α7、ML-α8 and ML-α9). The curved degree of the interface between Re-α4 and each adjacent ML-α is different, indicating the different swallowing degree. Fig. 7b shows the misorientations between Re-α4 and ML-α5, ML-α6 are both 2°, while those between Re-α4 and ML-α7, ML-α8, and ML-α9 are 8.5° (area 1), 17.5°(area 2) and 7.7° (area 3), respectively. Obviously, the recrystallized grain has the BOR and more curved interface with ML-α5 and ML-α6, but does not maintain the BOR with ML-α7, ML-α8 and ML-α9. This orientation relationship demonstrates the Re-α4 is a new grain.